HHS Public Access

Author manuscript

Environ Pollut. Author manuscript; available in PMC 2021 October 15.

Published in final edited form as:

Environ Pollut. 2021 October 15; 287: 117283. doi:10.1016/j.envpol.2021.117283.

Pharmacological inhibition of PAI-1 alleviates cardiopulmonary pathologies induced by exposure to air pollutants $PM_{2.5}$☆

Asish K. Ghosh[a,*], **Saul Soberanes**[b], **Elizabeth Lux**[a], **Meng Shang**[a], **Raul Piseaux Aillon**[b], **Mesut Eren**[a], **G.R. Scott Budinger**[b], **Toshio Miyata**[c], **Douglas E. Vaughan**[a]

[a]Feinberg Cardiovascular and Renal Research Institute, Northwestern University Feinberg School of Medicine, Chicago, IL, USA

[b]Pulmonary and Critical Care Division, Northwestern University Feinberg School of Medicine, Chicago, IL, USA

[c]United Centers for Advanced Research and Translational Medicine, Tohoku University, Miyagi, Japan

Abstract

Numerous studies have established that acute or chronic exposure to environmental pollutants like particulate matter (PM) leads to the development of accelerated aging related pathologies including pulmonary and cardiovascular diseases, and thus air pollution is one of the major global threats to human health. Air pollutant particulate matter 2.5 ($PM_{2.5}$)-induced cellular dysfunction impairs tissue homeostasis and causes vascular and cardiopulmonary damage. To test a hypothesis that elevated plasminogen activator inhibitor-1 (PAI-1) levels play a pivotal role in air pollutant-induced cardiopulmonary pathologies, we examined the efficacy of a drug-like novel inhibitor of PAI-1, TM5614, in treating $PM_{2.5}$-induced vascular and cardiopulmonary pathologies. Results from biochemical, histological, and immunohistochemical studies revealed that $PM_{2.5}$ increases the circulating levels of PAI-1 and thrombin and that TM5614 treatment completely abrogates these effects in plasma. $PM_{2.5}$ significantly augments the levels of pro-inflammatory cytokine interleukin-6 (IL-6) in bronchoalveolar lavage fluid (BALF), and this also can be reversed by TM5614, indicating its efficacy in amelioration of $PM_{2.5}$-induced increases in inflammatory and pro-thrombotic factors. TM5614 reduces $PM_{2.5}$-induced increased levels of inflammatory markers cluster of differentiation 107 b (Mac3) and phospho-signal transducer and activator of

---

☆This paper has been recommended for acceptance by J Jiayin Dai.

*Corresponding author. Asish K Ghosh, PhD, FAHA, Feinberg Cardiovascular and Renal Research Institute, Northwestern University Feinberg School of Medicine, Tarry 14-725, 303 East Chicago Ave, Chicago, IL 60611, USA. a-ghosh2@northwestern.edu (A.K. Ghosh).

Author's contributions

Asish K Ghosh: Conceptualization, Methodology, Investigation, Visualization, Analysis, Writing of Original Draft, Reviewing, Editing, Funding Acquisition; Saul Soberanes, Elizabeth LuX, Meng Shang, Raul PiseauX Aillon, Mesut Eren: Methodology, Investigation, Data collection, Reviewing, Data Analysis; G.R. Scott Budinger, Toshio Miyata, Douglas E Vaughan: Provided Valuable Resources, Conceptualization, Reviewing, Interpretation, Funding Acquisition.

Appendix A. Supplementary data

Supplementary data to this article can be found online at https://doi.org/10.1016/j.envpol.2021.117283.

Declaration of competing interest

The authors declare that they have no known competing financial interests or personal relationships that could have appeared to influence the work reported in this paper.

transcription-3 (pSTAT3), adhesion molecule vascular cell adhesion molecule 1 (VCAM1), and apoptotic marker cleaved caspase 3. Longer exposure to $PM_{2.5}$ induces pulmonary and cardiac thrombosis, but TM5614 significantly ameliorates $PM_{2.5}$-induced vascular thrombosis. TM5614 also reduces $PM_{2.5}$-induced increased blood pressure and heart weight. In vitro cell culture studies revealed that $PM_{2.5}$ induces the levels of PAI-1, type I collagen, fibronectin (Millipore), and sterol regulatory element binding protein-1 and 2 (SREBP-1 and SREBP-2), transcription factors that mediate profibrogenic signaling, in cardiac fibroblasts. TM5614 abrogated that stimulation, indicating that it may block $PM_{2.5}$-induced PAI-1 and profibrogenic signaling through suppression of SREBP-1 and 2. Furthermore, TM5614 blocked $PM_{2.5}$-mediated suppression of nuclear factor erythroid related factor 2 (Nrf2), a major antioxidant regulator, in cardiac fibroblasts. Pharmacological inhibition of PAI-1 with TM5614 is a promising therapeutic approach to control air pollutant $PM_{2.5}$-induced cardiopulmonary and vascular pathologies.

Keywords

Air pollutants; Particulate matter $PM_{2.5}$; PAI-1; TM5614; Vascular thrombosis

1. Introduction

Air pollution-associated toxicity is a major threat to human health. Exposure to air pollutants leads to development of pulmonary and cardiovascular disease-related morbidity and mortality. Environmental pollutants like ozone, nitrogen oxide, and particulate matter (PM) induce oxidative stress, which leads to cardiopulmonary vascular diseases (CPVDs) including thrombosis, hypertension, arteriosclerosis, arrhythmias, and myocardial infarction —affecting millions of people worldwide (Du et al., 2016; Bourdrel et al., 2017). PM is the most dangerous environmental pollutant, as these solid particles contain a wide variety of toxic substances including sulfates, nitrates, hydrocarbons, heavy metals, and bacteria. Based on its aerodynamic diameter, PM has been classified as coarse (PM_{10}), fine ($PM_{2.5}$), and ultrafine ($PM_{0.1}$) (Brook et al., 2004, 2010). The detrimental effects of PM on the cardiopulmonary/vascular system stem from chronic or acute exposure-induced oxidative stress and systemic inflammation, cellular dysfunction, and impaired tissue homeostasis (Brook et al., 2004, 2010; Nel, 2005; Simkhovich et al., 2009; Franchini and Mannucci, 2011; Budinger and Mutlu, 2011; Du et al., 2016; Bourdrel et al., 2017). While the acute effects of PM may be direct, involving rapid crossover from the lung epithelium into the circulation, the chronic effects of PM involve generation of pulmonary oxidative stress, systemic inflammation, and cellular dysfunction (Nelin et al., 2012; Robertson and Miller, 2018; Wu et al., 2019). With time, both direct and indirect effects of PM facilitate the onset and progression of CPVD pathologies. However, the exact molecular mechanism by which environmental pollutants like $PM_{2.5}$ contribute to cardiopulmonary vascular diseases is not fully understood.

Plasminogen activator inhibitor-1 (PAI-1), a secretory protein that inhibits t-PA/uPA serine proteases, regulates the tissue fibrinolytic system, and its deregulation contributes to different diseases, including CPVDs like thrombosis and accelerated cellular senescence and aging (Westrick and Eitzman, 2007; Ghosh and Vaughan, 2012; Ghosh et al., 2016;

Vaughan et al., 2017; Sun et al., 2019). Here, we tested a hypothesis that elevation of PAI-1 plays a pivotal role in PM-induced CPVDs by inhibiting t-PA, increasing oxidative stress, and promoting cellular dysfunction and cardiopulmonary vascular injury; conversely, pharmacological inhibition of PAI-1 ameliorates PM-induced CPVDs. The strong rationale behind formulating this hypothesis comes from the previous reports that (i) the levels of PAI-1 are significantly elevated in oxidative stress-induced cardiac cells, (ii) elevated PAI-1 is a key determinant of premature cellular senescence and dysfunction in different pulmonary and cardiac cells, and (iii) pharmacological inhibition of PAI-1 effectively blocks oxidative stress-induced cellular dysfunction through suppression of key senescence mediators (Ghosh et al., 2016; Vaughan et al., 2017; Sun et al., 2019). In addition, the levels of PAI-1 are significantly elevated in bronchoalveolar lavage fluid (BALF) in mice, and in lung and heart tissues from rats, exposed to $PM_{2.5}$ and are associated with inflammation and apoptosis (Upadhyay et al., 2010; Budinger et al., 2011). These findings strongly predict a therapeutically relevant function of PAI-1 inhibition in preventing $PM_{2.5}$-induced CPVDs. In this study, we tested the efficacy of a novel drug-like small molecule inhibitor of PAI-1, TM5614, in amelioration of air pollutant $PM_{2.5}$-induced CPVD pathologies. The N-acylanthranilic acid derivative TM5614 is designed based on the structure of original compounds TM5001 and TM5007. TM5614 is a novel PAI-1 inhibitor with better oral bioavailability that selectively inhibits PAI-1 activity (Yamaoka et al., 2018; Yahata et al., 2021). Recently, TM5614 received FDA approval for clinical trial to assess the efficacy and safety of TM5614 for high-risk patients with severe COVID-19 symptoms (Clinical trials.gov Identifier: NCT04634799). The results of the present investigation reveal that pharmacological inhibition of PAI-1 in mice is associated with suppression of $PM_{2.5}$-induced inflammatory and prothrombotic factors and thus of CPVD pathologies including vascular thrombosis.

2. Materials and Methods

All data and supporting materials have been provided with the published article and in the data supplement.

2.1. Animal studies

Wild-type, PAI-1 heterozygous, and PAI-1 knockout C57BL/6 mice (9–12 weeks old) were used for this study. All mouse protocols were approved by the Northwestern University Animal Care and Use Committee. Wild-type male mice were divided into 4 groups. Group 1: mice were fed with regular chow and received 50 μl of phosphate-buffered saline (PBS as negative control) (25 μl, twice) by intratracheal instillation. Group 2: mice were fed with regular chow and received particulate matter 2.5 ($PM_{2.5}$ was suspended in 50 μl of sterile PBS) (the National Institutes of Standards and Technology, Gaithersburg, MD, USA; NIST SRM 1649) (50 μg-200μg/mouse; 50 μg or 100 μg or 200 μg in 50 μl PBS; 25 μl, twice) by intratracheal instillation. Doses of $PM_{2.5}$ were selected based on well-accepted published literature (Urich et al., 2009; Soberanes et al., 2009, Upadhyay et al., 2010, Budinger et al., 2011, Pei et al., 2016, Yang et al., 2019, Huang et al., 2019, Jeong et al., 2019). Group 3: mice were fed with chow containing TM5614 (10 mg/kg/day) (dose has been selected based on previous published reports using TM5614 molecule) (Yahata et al., 2021) for 6

days and then received PBS (25 μl, twice) and TM5614 chow. Group 4: mice were fed with chow containing TM5614 (10 mg/kg/day) for 6 days and then received $PM_{2.5}$ (50 or 200 μg/mouse in 50 μl PBS; 25 μl, twice) and TM5614 chow. After 24 h or 72 h (short-term exposure to $PM_{2.5}$: 50 or 200 μg/mouse or PBS in the presence or absence of TM5614) or after 4 weeks (long-term exposure to $PM_{2.5}$: 100 μg/mouse/week or PBS in the presence or absence of TM5614), mice were sacrificed and plasma and BALF (short-term exposure only) were collected and processed for biochemical analysis. For PAI-1 genetic deficiency study, batches of wild-type, PAI-1 heterozygous, and PAI-1 knockout male and female mice were fed with regular chow and treated either with $PM_{2.5}$ (50 μg/mouse/week for 4 weeks) or PBS as controls. Hearts and lungs from short-term exposed mice (72 h to study the early pathological events) and long-term-exposed mice (4 weeks to study late pathological events) were collected and used for histological and immunohistochemical analysis. In vivo experimental plan has been presented in Table 1 under A-D.

2.2. Measurement of PAI-1 and thrombin-antithrombin (TAT) complex levels in plasma

Plasma was collected from the 4 groups of wild-type mice, and 50 μl of TAT standard and each sample were used in duplicate for TAT assays using a mouse ELISA kit for TAT (cat no ab137994, Abcam). Similarly, PAI-1 standard and each plasma sample were used in duplicate for PAI-1 assays using a mouse PAI-1 ELISA kit (cat no ab197752, Abcam).

2.3. Measurement of IL-6 in BALF

BALF was collected from each of the 4 groups of mice after 24 h of treatment as indicated above, and 50 μl of IL-6 standard and each sample were used in duplicate for IL-6 protein measurement using a Quantikine IL-6 mouse ELISA kit (cat no M6000B, R&D).

2.4. Blood pressure and echocardiography

To monitor the effect of $PM_{2.5}$ exposure on blood pressure, both systolic and diastolic blood pressure were measured in conscious mice using a non-invasive tail-cuff system (CODA Non-Invasive Blood Pressure, Kent Scientific Corp.). Trans-thoracic two-dimensional M-mode echocardiography was performed using a Vevo 3100 device (FujiFilm VisualSonics Inc., Toronto, Canada) equipped with a MX550D transducer. Echocardiographic studies were performed following manufacturer's instruction (https://www.visualsonics.com/product/transducers/mx-series-transducers) after 4 weeks of $PM_{2.5}$ exposure. M-mode tracings were used to measure left ventricular (LV) wall thickness, LV dimensions, LV volume, and LV mass. Percent fractional shortening (% FS) and ejection fraction (% EF) were also determined. The mean value of at least 3–5 cardiac cycles was used to determine the measurements for each animal in all four groups. Post-mortem heart weight and body weight of each mouse in all four groups were recorded and compared.

2.5. Histology

Heart and lung tissues were collected and fixed in 10% formalin overnight at room temperature, followed by fixation in 70% ethanol at 4°C overnight, and then processed for embedding in paraffin. Paraffin-embedded heart and lung tissues were subjected to microtome sectioning and processed for histological analysis. For morphology studies, the

tissues were processed for hematoxylin and eosin (H&E) staining. The H&E staining of specimens was performed on a fully automated platform (Leica Autostainer XL) using Harris hematoxylin (Fisherbrand) and eosin (Leica). The levels of collagen deposition and thrombotic blood vessels in lung and heart tissues were determined by H&E and Masson trichrome staining. Photographs were taken with an Olympus DP71 camera. The levels of matrix deposition were estimated by Fiji-ImageJ software.

2.6. Immunohistochemistry

For immunohistochemical studies, formalin-fixed paraffin-embedded tissue sections (4 μm) were first deparaffinized on an automated platform (Leica Autostainer XL). After deparaffinization, slides were subjected to an antigen retrieval step. Tissue sections were incubated with specific primary antibody overnight at 4 ○C. The primary antibodies used in this study included cluster of differentiation 107 b (Mac3) (BD Biosciences), phospho-signal transducer and activator of transcription-3 (pSTAT3) (Cell Signaling), Cleaved Caspase 3 (Cell Signaling), vascular cell adhesion molecule 1 (VCAM1) (Abcam). Secondary antibody incubation and chromogenic reactions were performed using an automated system (Biocare Intellipath). After antibody staining, tissue sections were counterstained with hematoxylin. Slides were then coverslipped using a xylene-based mounting medium (Leica Micromount). Photographs were taken using a light microscope. The sum of several fields per lung and heart tissue from each mouse were used for staining intensity measurement using ImageJ software, and the levels of statistical significance were determined.

2.7. Cell cultures and treatment with $PM_{2.5}$ and TM5614

Primary cultures of human cardiac fibroblasts were grown in Dulbecco's Modified Eagle Medium (DMEM) containing 10% fetal bovine serum (FBS) and 1% penicillin and streptomycin. To test the efficacy of PAI-1 inhibitor TM5614 in suppression of $PM_{2.5}$-induced cardiac fibroblast dysfunction, confluent cultures of human cardiac fibroblasts were subcultured in 12-well clusters. After 24 h, media were replaced with 0.1% FBS-containing DMEM for 3 h. Cells were pretreated with TM5614 (10 μM) or DMSO (vehicle control) for 2 h followed by treatment with $PM_{2.5}$ (50 μg/ml) in triplicate for another 2 h. For the other set of experiments, cells were pretreated with TM5614 (10 μM) or DMSO in triplicate for 24 h. After 24 h, media were replaced with 0.1% FBS-containing DMEM and treated with TM5614 (10 μM) or DMSO and $PM_{2.5}$ (50 μg/ml) (dose selected based on published literature) (Liu et al., 2018; Zhu et al., 2018) in triplicate for another 24 h. In vitro experimental plan has been presented in Table 1 under E.

2.8. Preparation of cell lysates and Western blot analysis

At the end of treatment with $PM_{2.5}$ in the absence and presence of PAI-1 inhibitor TM5614, supernatants from control and treated wells were collected. The cell lysates were prepared using RIPA lysis buffer (25 mM Tris•HCl pH 7.6, 150 mM NaCl, 1% NP-40, 1% sodium deoxycholate, 0.1% SDS) (ThermoFisher Scientific) containing protease inhibitor cocktail (cOmplete) and phosphatase inhibitor cocktail (PhosSTOP) (Sigma). Cell lysates were pooled from 3 wells for each control and treatment group and equal amounts of protein were subjected to gel electrophoresis, transferred to PVDF membranes, and subjected to western blotting using antibodies against PAI-1 (Molecular Innovations, Inc.), type I collagen

(Southern Biotech), fibronectin (Millipore), sterol regulatory element binding protein-1 and 2 (SREBP1, SREBP2), nuclear factor erythroid related factor 2 (Nrf2) (Abcam), and α-tubulin (GenScript), with HRP-tagged corresponding secondary antibodies. The membranes were developed with enhanced chemiluminescence reagents (Luminata Forte, Millipore, Billerica, MA), and images of protein bands were captured using a BIO-RAD ChemiDoc XRS system (BIO-RAD, CA).

2.9. Statistical analysis

Data are presented as mean ± SEM. The significance of differences between controls and experimental groups was determined by statistical analysis using Student's t-test, where a value of $P < 0.05$ was considered statistically significant. Statistical analyses were performed with GraphPad Prism (GraphPad Software Inc., San Diego, CA).

3. Results

3.1. PAI-1 inhibitor TM5614 reduces $PM_{2.5}$ exposure-induced plasma levels of PAI-1 and thrombin in mice

Four groups of mice described in the Methods section were used in this study: group 1, controls; group 2, $PM_{2.5}$ only; group 3, TM5614 only; and group 4, TM5614 and $PM_{2.5}$. After 24 h or 72 h of $PM_{2.5}$ exposure, mice were sacrificed, and plasma was used for PAI-1 and TAT assays. The results revealed that exposure to $PM_{2.5}$ (50 μg/mouse) for 24 h increases the levels of PAI-1 significantly, and TAT complex insignificantly in plasma. Importantly, pretreatment of mice with PAI-1 inhibitor TM5614 completely abrogates the $PM_{2.5}$-induced increased levels of PAI-1 and TAT in plasma (Fig. 1A and B). Similarly, exposure to $PM_{2.5}$ (200 μg/mouse) for 72 h significantly stimulates the levels of TAT in plasma, and TM5614 abrogates that stimulation (Fig. 1C). These results indicate that PAI-1 inhibitor TM5614 is highly efficient in reduction of $PM_{2.5}$-induced PAI-1 and thrombin, which contribute to vascular pathologies like thrombosis.

3.2. PAI-1 inhibitor TM5614 significantly inhibits $PM_{2.5}$-induced IL-6 in BALF

BALF collected from the four groups of mice was used for determination of IL-6 levels as described in the Methods. Administration of $PM_{2.5}$ (50 μg/mouse) for 24 h significantly increases the levels of pro-inflammatory cytokine IL-6 in BALF and most importantly, $PM_{2.5}$ fails to stimulate the levels of IL-6 in mice fed with TM5614, indicating the efficacy of PAI-1 inhibitor TM5614 in amelioration of $PM_{2.5}$-induced lung inflammation (Fig. 1D). The levels of IL-6 in BALF from TM5614-treated (Group 3) and PBS control (Group 1) mice are not significantly increased ($p = 0.1301$).

3.3. PAI-1 inhibitor TM5614 alleviates $PM_{2.5}$-induced lung inflammation, apoptosis, and vascular pathologies

Wild-type mice were exposed to a single dose of $PM_{2.5}$ (200 μg/mouse). After 72 h, lung tissues were collected and processed for morphological analysis by H&E staining and immunohistochemical analysis using antibodies against inflammatory markers Mac3 and pSTAT3, apoptotic marker cleaved caspase 3, and adhesion molecule VCAM1. Morphologically, $PM_{2.5}$-exposed lungs (4 out of 7) are relatively denser compared to

PBS controls (1 out of 4) and importantly, TM5614 partially reverses the $PM_{2.5}$-induced lung morphological changes (Supplemental Figure s1, representative images are presented). Immunohistochemistry results revealed the presence of low levels of inflammation in PBS-treated lungs as expected in fluid instilled-lungs. However, administration of $PM_{2.5}$ increases the staining intensity of pSTAT3 and Mac3 compared to controls and mice treated with TM5614 alone. Treatment with PAI-1 inhibitor TM5614 modestly reduces $PM_{2.5}$-induced pSTAT3 without reaching statistical significance (representative images are presented in Fig. 2A and quantitative data are shown in Fig. 2B) and significantly reduces the Mac3 (representative images are presented in Fig. 2C, and quantitative data are shown in Fig. 2D) levels in lung tissues. These results are consistent with our observation that $PM_{2.5}$ induces the level of pro-inflammatory cytokine IL-6 in BALF and TM5614 completely abrogates the $PM_{2.5}$-induced increased levels of IL-6 in lungs.

Exposure to $PM_{2.5}$ for 72 h significantly increases the levels of cleaved caspase 3 positivity in lungs (Fig. 3A, representative image from each group; quantitative data are shown in Fig. 3B). Importantly, TM5614 treatment reduces the levels of cleaved caspase 3 positivity in lungs. Next, we determined the levels of adhesion molecule VCAM1, known to be involved in inflammation and vascular dysfunction, in $PM_{2.5}$-exposed murine lungs. Exposure to $PM_{2.5}$ induces the levels of VCAM1, consistent with the previous observation that $PM_{2.5}$-induced stress increases VCAM1 in endothelial cells (Rui et al., 2016; Cui et al., 2019). Most importantly, TM5614 prevents $PM_{2.5}$-induced induction of VCAM1 (representative images are presented in Fig. 4A from each group; quantitative data are shown in Fig. 4B). Collectively, these results indicate that pharmacological inhibition of PAI-1 is an ideal approach to control air pollutant-induced inflammation and cellular apoptosis in murine lungs and that small molecule TM5614 effectively prevents air pollutant-induced lung pathological events.

3.4. Effect of PAI-1 inhibitor TM5614 on $PM_{2.5}$-induced cardiac inflammation and apoptosis

Hearts collected from the four groups of mice were processed for H&E staining and immunohistochemical analysis using antibodies against pSTAT3, Mac3, cleaved caspase 3, and VCAM1. There were no morphological changes in $PM_{2.5}$-exposed hearts (Supplemental Figure s2). Immunohistochemistry results revealed that exposure to $PM_{2.5}$ (200 μg/mouse) for 72 h modestly increases the levels of cleaved caspase 3 in myocardial tissues and that TM5614 treatment reduces the levels of cleaved caspase 3 without attaining statistical significance (Fig. 5A, representative image from each group; quantitative data are shown in Fig. 5B). The levels of $PM_{2.5}$-induced apoptotic cells in hearts are lower compared to lungs. While administration of $PM_{2.5}$ significantly increases cardiac inflammation as evidenced by increased Mac3 staining, TM5614 modestly reduces inflammation (Fig. 5C, representative image from each group; quantitative data are shown in Fig. 5D). There is no difference in the levels of pSTAT3 in cardiac tissues derived from control and treated mice (Supplemental Figure s3A, representative image of each group, and quantitative data are shown in Figure s3B). While exposure to $PM_{2.5}$ modestly stimulates the levels of VCAM1 in myocardial tissues, in the TM5614-treated mice, $PM_{2.5}$ fails to stimulate adhesion molecule VCAM1 (Fig. 6A, representative image from each group; quantitative data are shown in Fig. 6B).

These results signify the efficacy of PAI-1 inhibitor TM5614 in suppression of air pollutant-induced cardiovascular pathologies.

3.5. Effect of long-term exposure to $PM_{2.5}$ on blood pressure, cardiac hypertrophy, and cardiac matrix remodeling

Mice were divided into 4 groups. In Group1, mice were fed with regular chow and received PBS. Group 2, mice were fed with regular chow and received $PM_{2.5}$ (100 μg/mouse/once per week for 4 weeks). Group 3, mice were fed with chow containing TM5614 (10 mg/kg) for 6 days and then received PBS for 4 weeks. Group 4, mice were fed with chow containing TM5614 (10 mg/kg) for 6 days and then received $PM_{2.5}$ (100 μg/mouse/once per week for 4 weeks). At the end of the 4 weeks, blood pressure was determined, and each mouse was subjected to echocardiography. The results revealed that 4 weeks of $PM_{2.5}$ exposure increases systolic pressure non-significantly and diastolic blood pressure significantly. Importantly, treatment of mice with PAI-1 inhibitor TM5614 reduces the $PM_{2.5}$-induced blood pressure increase (Supplemental Figure s4A,B). Analysis of echocardiography data revealed that there is no significant differences in EF, FS, left ventricular anterior or posterior wall thickness-systolic or diastolic (LVAWs, LVAWd, LVPWs and LVPWd) within control and treated groups (data not shown). Post-mortem heart weight analysis reveals that $PM_{2.5}$ (100 μg/mouse once per week for 4 weeks) induces cardiac hypertrophy based on increased heart weight/body weight ratio and that TM5614 decreases the $PM_{2.5}$-induced cardiac hypertrophy (Supplemental Figure s4C). Collectively, these results suggest that TM5614 is effective in amelioration of $PM_{2.5}$-induced cardiac pathologies including hypertension and cardiac hypertrophy. However, $PM_{2.5}$ fails to stimulate fibrogenesis in heart tissue after 4 weeks of treatment (100 μg once per week for 4 weeks) (data not shown).

3.6. PAI-1 inhibitor TM5614 reduces long-term $PM_{2.5}$ exposure-induced pulmonary and cardiac thrombosis in mice

Mice were divided into 4 groups and treated for 4 weeks as described above. At the end of treatment, mice were sacrificed, and heart and lungs were collected. Lung and heart tissues were processed for H&E staining and Masson's trichrome staining. Exposure to $PM_{2.5}$ for 4 weeks significantly induces pulmonary thrombogenesis in mice (incidence of thrombus formation: 4 out of 7) compared to PBS controls (incidence of thrombus formation: 0 out of 4) and mice treated with TM5614 alone (incidence of thrombus formation: 0 out of 5). Most importantly, $PM_{2.5}$ failed to induce pulmonary thrombosis in mice pretreated with PAI-1 inhibitor TM5614 (incidence of thrombus formation: 0/4) (Fig. 7, representative image of each group). This result is highly significant, as it clearly indicates the beneficial effect of PAI-1 inhibitor TM5614 in improving vascular thrombosis, a major pulmonary pathology, in mice exposed to air pollutant $PM_{2.5}$. However, $PM_{2.5}$ fails to stimulate the pulmonary fibrogenesis significantly after 4 weeks of treatment (Supplemental Figure s5A,B).

Analysis of hearts from each group revealed that longer exposure to $PM_{2.5}$ modestly induces cardiac thrombosis in mice, to a lesser extent than in lungs. However, $PM_{2.5}$ failed to induce cardiac thrombosis in mice pretreated with PAI-1 inhibitor TM5614 (Supplemental Figure s6). These results are consistent with our observation that $PM_{2.5}$ induces the expression of PAI-1 and thrombin, the major contributors to thrombogenesis, and that TM5614 completely

abrogates the $PM_{2.5}$-induced increased levels of PAI-1 and thrombin in plasma (Fig. 1). Additionally, these results further indicate that PAI-1 is an ideal druggable target for the treatment of air pollutant-induced cardiopulmonary pathologies, including vascular thrombosis.

3.7. PAI-1 heterozygous mice are partly protected from $PM_{2.5}$-induced pulmonary thrombosis

As a complementary study to pharmacological inhibition of PAI-1 and its beneficial effect on air pollutant-induced cardiopulmonary and vascular pathologies, next we investigated the effects of haplo- and complete genetic deficiency of PAI-1 on air pollutant $PM_{2.5}$-induced cardiopulmonary pathologies. Wild-type, PAI-1 heterozygous, and PAI-1 knockout mice were treated with $PM_{2.5}$ (50 μg/mouse/week for 4 weeks) or PBS as a control. All mice were fed with regular chow. Four weeks of $PM_{2.5}$ exposure induces pulmonary thrombosis in both wild-type and PAI-1 knockout mice, indicating complete deficiency of PAI-1 does not protect against developing $PM_{2.5}$-induced pulmonary pathologies. Interestingly, PAI-1 heterozygous mice are partially protected from $PM_{2.5}$-induced pulmonary thrombotic pathogenesis, indicating that, like pharmacological inhibition of PAI-1, PAI-1 haplodeficiency, but not complete absence of PAI-1, is beneficial for air pollutant-induced pulmonary pathologies (Supplemental Figure s7). However, we did not observe any difference in pulmonary matrix remodeling in $PM_{2.5}$-treated wild-type, PAI-1 heterozygous, and knockout groups as evidenced by Masson's trichrome staining (data not shown).

3.8. TM5614 reduces $PM_{2.5}$-induced cellular stresses and abnormalities

Previous reports suggest that $PM_{2.5}$ can enter into the systemic circulation and affects cardiovascular system (Nelin et al., 2012). As $PM_{2.5}$ is a known inducer of reactive oxygen species (ROS), TGF-β, and matrix remodeling, and fibroblasts are the major contributing cell type in matrix protein production, we have developed an in vitro model system to study the effects of $PM_{2.5}$ on cellular processes in cardiac fibroblasts and the efficacy of TM5614 in ameliorating $PM_{2.5}$-induced cellular abnormalities. Our results showed that $PM_{2.5}$ modestly induces the levels of PAI-1, type I collagen, and fibronectin and that TM5614 reduces the $PM_{2.5}$-induced stimulation of these fibrogenic factors (Fig. 8A–C). The $PM_{2.5}$-induced stimulation of PAI-1 and its normalization by TM5614 in vitro is consistent with the in vivo observation on plasma levels of PAI-1 in $PM_{2.5}$- and TM5614-treated mice (Fig. 1). As SREBP1, a basic-helix-loop-helix leucine zipper family transcription factor, mediates profibrogenic signaling and fibrogenesis (Chen et al., 2014), and air pollutants induce the expression of SREBP1 (Yan et al., 2020), we measured the levels of SREBP1 and SREBP2 in control, $PM_{2.5}$-, and TM5614-treated cardiac fibroblasts. Interestingly, $PM_{2.5}$ induces the expression of SREBP1/2 in human cardiac fibroblasts and most importantly, TM5614 completely abrogates that stimulation, indicating that TM5614 effectively blocks $PM_{2.5}$-induced profibrogenic signaling through suppression of SREBP1 and SREBP2 (Fig. 8A). As $PM_{2.5}$ induces reactive oxygen species (Liu et al., 2018) and Nrf2, a basic leucine zipper (bZip) transcription factor, is a master regulator of antioxidant genes and signaling (Vomund et al., 2017), we measured the effect of $PM_{2.5}$ on Nrf2 expression in human cardiac fibroblasts and the efficacy of TM5614 in normalizing the Nrf2 expression. Our

results revealed that $PM_{2.5}$ reduces the levels of Nrf2 in cardiac fibroblasts and importantly, that TM5614 reverses the suppression of Nrf2 by $PM_{2.5}$ (Fig. 8C). Collectively, these in vitro results indicate the efficacy of PAI-1 inhibitor TM5614 in improvement of cardiac cellular stresses and abnormalities induced by exposure to air pollutant $PM_{2.5}$.

4. Discussion

Environmental pollution is a global threat to organismal growth and health. Short-term or long-term exposure to environmental pollutants like PM causes devastating CPVDs. CPVDs including pulmonary inflammation, vascular dysfunction, hypertension, arteriosclerosis, arrhythmias, and myocardial infarction cause an estimated 60–80% of environmental pollutant-associated deaths worldwide (Brook et al., 2004, 2010; Nel, 2005; Simkhovich et al., 2009; Franchini and Mannucci, 2011; Budinger and Mutlu, 2011; Du et al., 2016; Bourdrel et al., 2017). However, the underlying molecular basis of PM-induced CPVDs is not well understood, and an effective therapeutic approach to block PM-induced CPVD-related pathologies is not available. As exposure to environmental pollutants deregulates the plasminogen activator system (Upadhyay et al., 2010; Budinger et al., 2011), and PAI-1 plays pivotal roles in initiation and progression of CPVDs (Westrick and Eitzman, 2007; Ghosh and Vaughan, 2012; Ghosh et al., 2016; Vaughan et al., 2017; Sun et al., 2019), we initiated the present study in order to delineate the role of PAI-1 in air pollutant $PM_{2.5}$-induced CPVD-related pathologies, and assess the potential of PAI-1 as a druggable target for CPVD therapy. Using the small molecule inhibitor TM5614, which targets PAI-1, and mouse strains with PAI-1 haplo- or complete deficiency, the present study demonstrated that PAI-1 plays a key role in air pollutant $PM_{2.5}$-induced CPVD pathologies and that pharmacological inhibition of PAI-1 ameliorates $PM_{2.5}$-induced CPVD pathologies.

In this study, we demonstrated that short-term exposure to air pollutant $PM_{2.5}$ increases the levels of pro-inflammatory and prothrombotic PAI-1 and thrombin in plasma and inflammatory cytokine IL-6 in lungs, consistent with previous observations (Budinger et al., 2011). The levels of TAT complex serve as an indicator of coagulation activation. Thrombin is a serine protease that converts soluble fibrinogen to an insoluble fibrous protein, fibrin that polymerizes and becomes a key component of blood clots. Antithrombin, an endogenous inhibitor of thrombin, forms the TAT complex with thrombin. As thrombin is highly unstable and has a short half-life in plasma, the TAT complex is measured as an indicator of thrombin levels and activation of coagulation that contributes to thrombosis (Chen et al., 2019).

Most importantly, here we have presented data showing that the stimulation of plasma levels of PAI-1 and thrombin, and BALF levels of IL-6 in air pollutant-exposed mice is abrogated by treatment with PAI-1 inhibitor TM5614. The elevated levels of PAI-1 and IL-6 clearly indicate increased inflammation by exposure to air pollutant $PM_{2.5,}$ and early inflammation plays a pivotal role in the development of downstream inflammatory signals and organ pathologies, especially in the lungs and cardiovascular system, including vascular occlusion and disruption of lung and heart tissue homeostasis (Fig. 9). Suppression of IL-6 by PAI-1 inhibitor TM5614 can be explained in the light of previous observations made by Kubala and colleagues, who demonstrated that while elevated PAI-1 stimulates the levels of IL-6

and activates downstream pSTAT3, depletion of PAI-1 is associated with down-regulation of IL-6 and pSTAT3 activation in response to inflammatory signals (Kubala et al., 2018).

Next, we investigated the effect of short-term exposure to $PM_{2.5}$ on lung and heart inflammation and apoptosis and showed that the lung morphology is abnormal in several $PM_{2.5}$-exposed mice (200 μg/mouse) in terms of its tissue density, consistent with previous observations that $PM_{2.5}$ causes damage in lung morphological structure (Urich et al., 2009; Budinger et al., 2011; Yang et al., 2019). These results indicate that acute exposure to air pollutant is able to damage lung tissue architecture. However, in the presence of PAI-1 inhibitor TM5614, $PM_{2.5}$ fails to induce pulmonary tissue damage. Furthermore, TM5614 reduces air pollutant $PM_{2.5}$-induced inflammation, apoptosis, and vascular dysfunction as evidenced by the decreased levels of inflammation- and apoptosis-associated factors in lungs derived from mice exposed to $PM_{2.5}$ in the presence of TM5614. Similarly, TM5614 is also effective in suppression of $PM_{2.5}$-induced modestly elevated inflammatory and apoptotic events in murine hearts. These results signify that pharmacological neutralization of $PM_{2.5}$-induced PAI-1 is an effective approach for suppression of early events of air pollutant-induced cardiovascular and pulmonary pathological events. Previous studies demonstrated that $PM_{2.5}$ induces the levels of PAI-1 (Upadhyay et al., 2010; Budinger et al., 2011), and that elevated PAI-1 plays a key role in a number of subclinical and clinical pathologies, including inflammation, multi-organ fibrosis, atherosclerosis, insulin resistance, obesity, and multi-morbidities (Westrick and Eitzman, 2007; Cesari et al., 2010; Ghosh and Vaughan, 2012; Vaughan et al., 2017). The elevated PAI-1 may also contribute to cellular apoptosis in a context-dependent manner. For example, the elevated PAI-1 in alveolar type II cells derived from idiopathic pulmonary fibrosis patients is associated with elevated levels of cleaved caspase 3 and thus increased apoptosis (Marudamuthu et al., 2015). Therefore, pharmacological suppression or neutralization of PAI-1 is an ideal approach to control pathological/sustained inflammation and disease development like air pollutant-induced increased inflammation and apoptosis-driven cardiopulmonary diseases.

The most notable observation we made in the present study is the induction of significant levels of pulmonary and, to a lesser degree, cardiac vascular thrombosis in mice exposed to air pollutant $PM_{2.5}$, and that air pollutant exposure fails to develop pulmonary and cardiac thrombosis in the mice treated with PAI-1 inhibitor TM5614. This result is consistent with our observation that TM5614 significantly reduces $PM_{2.5}$-induced increased levels of inflammation and prothrombotic mediators IL-6, PAI-1, and thrombin. It is important to mention that inflammation-associated increased levels of inflammatory mediators like circulatory IL-6, PAI-1, and VCAM-1in the vascular wall are known key contributors to endothelial dysfunction, and vascular remodeling that leads to the initiation and progression of cardiovascular pathologies including hypertension and cardiac hypertrophy (reviewed in Savio et al., 2011). Furthermore, normalization of $PM_{2.5}$-induced increased blood pressure and heart weight by TM5614 treatment are also significant in the context of the pivotal role of PAI-1 in $PM_{2.5}$-induced vascular pathologies. In this context, it is important to note that previous studies implicated PM and higher levels of PAI-1 in high blood pressure (Brook and Rajagopalan, 2009; Peng et al., 2017). Like wild-type mice, several PAI-1 knockout mice also developed pulmonary thrombosis upon longer exposure to air pollutant $PM_{2.5}$. Interestingly, PAI-1 haplodeficient mice exposed to $PM_{2.5}$ are partly protected from

developing pulmonary thrombosis, indicating that, like pharmacological inhibition of PAI-1, partial genetic deficiency of PAI-1 or low levels of PAI-1 are beneficial for organisms exposed to air pollutants. Therefore, it is apparent that normalization of the levels of PAI-1, but not complete depletion, is favorable to prevent air pollutant-induced pulmonary pathologies. Further studies are necessary to understand the underlying molecular basis. Although previous reports suggested significant cardiac matrix remodeling in mice and rats in response to exposure to air pollution (Xu et al., 2019; Yue et al., 2019; Sun et al., 2020), under our experimental setup (100 μg/once/week/4 weeks), we did not observe any significant change in collagen deposition in $PM_{2.5}$-exposed murine lungs and hearts. However, our in vitro study showed up-regulation of profibrogenic signal transducers and matrix proteins in cardiac fibroblasts exposed to $PM_{2.5,}$ and importantly, TM5614 is effective in the suppression of these $PM_{2.5}$-induced profibrogenic responses. Further studies are required to investigate the effect of $PM_{2.5}$ exposure with an increased number of doses/week for 3–6 months on pulmonary and cardiac pathological matrix remodeling and whether TM5614 can effectively block $PM_{2.5}$-induced pulmonary and cardiac fibrogenesis on that time-scale. Together, these results signify the pivotal role of PAI-1 in air pollutant-induced cardiopulmonary vascular pathologies and establish the potential therapeutic efficacy of PAI-1 inhibitor TM5614, an FDA-approved drug for clinical trials of other PAI-1 related pathologies, in amelioration of air pollutant exposure-mediated cardiopulmonary pathologies.

In search of cellular and molecular events induced by exposure to air pollutant $PM_{2.5}$, we studied the effects of $PM_{2.5}$ on cultured human cardiac fibroblasts in the presence and absence of TM5614. The rationale behind using cardiac fibroblasts in this cellular model study comes from previous experimental demonstrations that $PM_{2.5}$ can enter into the systemic circulations and thus directly affects heart and blood vascular system (reviewed in Nelin et al., 2012). The in vitro results suggest that air pollutant $PM_{2.5}$ modestly induces profibrogenic markers and regulators, namely profibrogenic PAI-1, matrix protein collagen, and transcriptional regulators SREBP1 and SREBP2; and most importantly, that PAI-1 inhibitor efficiently blocks air pollutant-induced increases in PAI-1, profibrogenic regulators, and target matrix proteins. The rescue of $PM_{2.5}$-induced suppression of Nrf2 levels by TM5614 is interesting, as it clearly indicates that suppression of Nrf2, a major transcriptional regulator of antioxidant genes, and augmentation of oxidative stress by $PM_{2.5}$ can be prevented by pharmacological inhibition of PAI-1. This result is consistent with our previous observations showing PAI-1 inhibition is associated with the rescue of homocysteine-mediated suppression of the antioxidant regulator Nrf2 (Sun et al., 2019), and of doxorubicin-mediated suppression of antioxidant catalase (Ghosh et al., 2016), as well as with prevention of accelerated cellular aging.

5. Conclusion

The present preclinical study establishes that PAI-1 is a potential druggable target for the treatment of air pollutant $PM_{2.5}$-induced cardiopulmonary vascular pathologies including inflammation, thrombosis, hypertension, and cardiac hypertrophy. Most importantly, here we demonstrate that TM5614, a drug-like small molecule inhibitor of PAI-1, effectively ameliorates these cardiopulmonary vascular pathologies by suppression of air pollutant

$PM_{2.5}$-induced mediators of inflammation, prothrombotic factors, profibrogenic regulators, and by rescuing $PM_{2.5}$-induced suppression of a key antioxidant regulator (Model depicting the $PM_{2.5}$-induced signaling pathway and feed-back loop in Fig. 9 which is based on results from the present study and previously published articles). Further in vitro studies are needed to test the efficacy of TM5614 in amelioration of air pollutant-induced other signaling pathways involved in cardiopulmonary vascular pathologies, including inflammatory signaling, canonical or non-canonical TGF-β signaling, and pro-apoptotic signaling pathways in endothelial cells and macrophages. Future expansion of the present study will be helpful to design clinical trials of TM5614 for the treatment of air pollutant-induced CPVDs.

Supplementary Material

Refer to Web version on PubMed Central for supplementary material.

Acknowledgments

We thank Northwestern University's Mouse Histology and Phenotyping Laboratory for technical support.

Source of funding

This work is supported by the American Heart Association-Innovative Project Award (18IPA34170365) and by a grant from the National Institutes of Health (5R01HL051387).

References

Bourdrel T, Bind MA, Béjot Y, Morel O, Argacha JF, 2017. Cardiovascular effects of air pollution. Arch. Cardiovasc. Dis. 110, 634–642. [PubMed: 28735838]

Brook RD, Franklin B, Cascio W, Hong Y, Howard G, Lipsett M, Luepker R, Mittleman M, Samet J, Smith SC Jr., Tager I, 2004. Expert panel on population and prevention science of the American heart association. Air pollution and cardiovascular disease: a statement for healthcare professionals from the expert panel on population and prevention science of the American heart association. Circulation109, 2655–2671. [PubMed: 15173049]

Brook RD, Rajagopalan S, 2009. Particulate matter, air pollution, and blood pressure. J Am Soc Hypertens3, 332–350. [PubMed: 20409976]

Brook RD, Rajagopalan S, Pope CA 3rd, Brook JR, Bhatnagar A, Diez-Roux AV, Holguin F, Hong Y, Luepker RV, Mittleman MA, Peters A, Siscovick D, Smith SC Jr., Whitsel L, Kaufman JD, 2010. American heart association council on epidemiology and prevention, council on the kidney in cardiovascular disease, and council on nutrition, physical activity and metabolism. Particulate matter air pollution and cardio-vascular disease: an update to the scientific statement from the American heart association. Circulation121, 2331–2378. [PubMed: 20458016]

Budinger GR, McKell JL, Urich D, Foiles N, Weiss I, Chiarella SE, Gonzalez A, Soberanes S, Ghio AJ, Nigdelioglu R, Mutlu EA, Radigan KA, Green D, Kwaan HC, Mutlu GM, 2011. Particulate matter-induced lung inflammation increases systemic levels of PAI-1 and activates coagulation through distinct mechanisms. PloS One6, e18525. [PubMed: 21494547]

Budinger GR, Mutlu GM, 2011. Update in environmental and occupational medicine 2010. Am. J. Respir. Crit. Care Med. 183, 1614–1619. [PubMed: 21693716]

Carrim N, Arthur JF, Hamilton JR, Gardiner EE, Andrews RK, Moran N, Berndt MC, Metharom P, 2015. Thrombin-induced reactive oxygen species generation in platelets: a novel role for protease-activated receptor 4 and GPIbα. Redox Biol6, 640–647. [PubMed: 26569550]

Cesari M, Pahor M, Incalzi RA, 2010. Plasminogen activator inhibitor-1 (PAI-1): a key factor linking fibrinolysis and age-related subclinical and clinical conditions. Cardiovasc. Ther. 28, e72–91. [PubMed: 20626406]

Chen D, Dorling A, 2009. Critical roles for thrombin in acute and chronic inflammation. J. Thromb. Haemostasis7 (Suppl. 1), 122–126. [PubMed: 19630783]

Chen G, Wang T, Uttarwar L, vanKrieken R, Li R, Chen X, Gao B, Ghayur A, Margetts P, Krepinsky JC, 2014. SREBP-1 is a novel mediator of TGFβ1 signaling in mesangial cells. J. Mol. Cell Biol. 6, 516–530.

Chen Q, Shou W, Wu W, Wang G, Cui W, 2019. Performance evaluation of thrombomodulin, thrombin-antithrombin complex, plasmin-α2-antiplasmin complex, and t-PA: PAI-1 complex. J. Clin. Lab. Anal. 33, e22913. [PubMed: 31090232]

Cui A, Xiang M, Xu M, Lu P, Wang S, Zou Y, Qiao K, Jin C, Li Y, Lu M, Chen AF, Chen S, 2019. VCAM-1-mediated neutrophil infiltration exacerbates ambient fine particle-induced lung injury. Toxicol. Lett. 302, 60–74. [PubMed: 30447258]

Danckwardt S, Hentze MW, Kulozik AE, 2013. Pathologies at the nexus of blood coagulation and inflammation: thrombin in hemostasis, cancer, and beyond. J. Mol. Med. 91, 1257–1271. [PubMed: 23955016]

Du Y, Xu X, Chu M, Guo Y, Wang J, 2016. Air particulate matter and cardiovascular disease: the epidemiological, biomedical and clinical evidence. J. Thorac. Dis. 8, E8–E19. [PubMed: 26904258]

Foley HH, Conway EM, 2016. Cross talk pathways between coagulation and inflammation. Circ. Res. 118, 1392–1408. [PubMed: 27126649]

Franchini M, Mannucci PM, 2011. Thrombogenicity and cardiovascular effects of ambient air pollution. Blood118, 2405–2412. [PubMed: 21666054]

Ghosh AK, Rai R, Park KE, Eren M, Miyata T, Wilsbacher LD, Vaughan DE, 2016. A small molecule inhibitor of PAI-1 protects against doxorubicin-induced cellular senescence. Oncotarget7, 72443–72457. [PubMed: 27736799]

Ghosh AK, Vaughan DE, 2012. PAI-1 in tissue fibrosis. J. Cell. Physiol. 227, 493–507. [PubMed: 21465481]

Hsieh CY, Sheu JR, Yang CH, Chen WL, Tsai JH, Chung CL, 2019. Thrombin upregulates PAI-1 and mesothelial-mesenchymal transition through PAR-1 and contributes to tuberculous pleural fibrosis. Int. J. Mol. Sci. 20, 5076.

Huang K, Shi C, Min J, Li L, Zhu T, Yu H, Deng H, 2019. Study on the mechanism of curcumin regulating lung injury induced by outdoor fine particulate matter (PM2.5). Mediat. Inflamm. 2019, 8613523.

Jeong S, Park SA, Park I, Kim P, Cho N-H, Hyun JW, Hyun Y-M, 2019. $PM_{2.5}$ exposure in the respiratory system induces distinct inflammatory signaling in the lung and the liver of mice. J. Immunol. Res. 2019, 348684110.1155/2019/3486841, 11 pages. [PubMed: 31871955]

Kubala MH, Punj V, Placencio-Hickok VR, Fang H, Fernandez GE, Sposto R, DeClerck YA, 2018. Plasminogen activator inhibitor-1 promotes the recruitment and polarization of macrophages in cancer. Cell Rep. 25, 2177–2191. [PubMed: 30463014]

Liu CW, Lee TL, Chen YC, Liang C-J, Wang S-H, Lue J-H, Tsai J-S, Lee S-W, Chen S-H, Yang Y-F, Chuang T-Y, Chen Y-L, 2018. $PM_{2.5}$-induced oxidative stress increases intercellular adhesion molecule-1 expression in lung epithelial cells through the IL-6/AKT/STAT3/NF-κB-dependent pathway. Part. Fibre Toxicol. 15, 4. [PubMed: 29329563]

Lopez JJ, Salido GM, Gomez-Arteta E, Rosado JA, Pariente JA, 2007. Thrombin induces apoptotic events through the generation of reactive oxygen species in human platelets. J. Thromb. Haemostasis5, 1283–1291. [PubMed: 17567446]

Margetic S, 2012. Inflammation and haemostasis. Biochem. Med. 22, 49–62.

Marudamuthu AS, Shetty SK, Bhandary YP, Karandashova S, Thompson M, Sathish V, Florova G, Hogan TB, Pabelick CM, Prakash YS, Tsukasaki Y, Fu J, Ikebe M, Idell S, Shetty S, 2015. Plasminogen activator inhibitor-1 suppresses profibrotic responses in fibroblasts from fibrotic lungs. J. Biol. Chem. 290, 9428–9441. [PubMed: 25648892]

Mittal M, Siddiqui MR, Tran K, Reddy SP, Malik AB, 2014. Reactive oxygen species in inflammation and tissue injury. Antioxidants Redox Signal. 20, 1126–1167.

Nelin TD, Joseph AM, Gorr MW, Wold LE, 2012. Direct and indirect effects of particulate matter on the cardiovascular system. Toxicol. Lett. 208, 293–299. [PubMed: 22119171]

Nel A, 2005. Atmosphere. Air pollution-related illness: effects of particles. Science308, 804–806. [PubMed: 15879201]

Pei Y, Jiang R, Zou Y, Wang Y, Zhang S, Wang G, Zhao J, Song W, 2016. Effects of fine particulate matter (PM2.5) on systemic oxidative stress and cardiac function in ApoE$^{-/-}$ mice. Int. J. Environ. Res. Publ. Health13, 484.

Peng H, Yeh F, de Simone G, Best LG, Lee ET, Howard BV, Zhao J, 2017. Relationship between plasma plasminogen activator inhibitor-1 and hypertension in American Indians: findings from the strong heart study. J. Hypertens. 35, 1787–1793. [PubMed: 28379891]

Rabiet MJ, Plantier JL, Dejana E, 1994. Thrombin-induced endothelial cell dysfunction. Br. Med. Bull. 50, 936–945. [PubMed: 7804740]

Robertson S, Miller MR, 2018. Ambient air pollution and thrombosis. Part. Fibre Toxicol. 3 (15), 1.

Rui W, Guan L, Zhang F, Zhang W, Ding W, 2016. PM2.5-induced oxidative stress increases adhesion molecules expression in human endothelial cells through the ERK/AKT/NF-κB-dependent pathway. J. Appl. Toxicol. 36, 48–59. [PubMed: 25876056]

Savoia C, Sada L, Zezza L, Pucci L, Lauri FM, Befani A, Alonzo A, Volpe M, 2011. Vascular inflammation and endothelial dysfunction in experimental hypertension. Int. J. Hypertens. 2011, 281240. [PubMed: 21915370]

Simkhovich BZ, Kleinman MT, Kloner RA, 2009. Particulate air pollution and coronary heart disease. Curr. Opin. Cardiol. 24, 604–609. [PubMed: 19696664]

Soberanes S, Urich D, Baker CM, Burgess Z, Chiarella SE, Bell EL, Ghio AJ, De Vizcaya-Ruiz A, Liu J, Ridge KM, Kamp DW, Chandel NS, Schumacker PT, Mutlu GM, Budinger GR, 2009. Mitochondrial complex III-generated oxidants activate ASK1 and JNK to induce alveolar epithelial cell death following exposure to particulate matter air pollution. J. Biol. Chem. 284, 2176–2186. [PubMed: 19033436]

Sun B, Shi Y, Li Y, Jiang J-j., Liang S, Duan J, Sun Z, 2020. Short-term PM2.5 exposure induces sustained pulmonary fibrosis development during post-exposure period in rats. J. Hazard Mater. 385, 121566. [PubMed: 31761645]

Sun T, Ghosh AK, Eren M, Miyata T, Vaughan DE, 2019. PAI-1 contributes to homocysteine-induced cellular senescence. Cell. Signal. 64, 109394. [PubMed: 31472244]

Upadhyay S, Ganguly K, Stoeger T, Semmler-Bhenke M, Takenaka S, Kreyling WG, Pitz M, Reitmeir P, Peters A, Eickelberg O, Wichmann HE, Schulz H, 2010. Cardiovascular and inflammatory effects of intratracheally instilled ambient dust from Augsburg, Germany, in spontaneously hypertensive rats (SHRs). Part. Fibre Toxicol. 7, 27. [PubMed: 20920269]

Urich D, Soberanes S, Burgess Z, Chiarella SE, Ghio AJ, Ridge KM, Kamp DW, Chandel NS, Mutlu GM, Budinger GR, 2009. Proapoptotic Noxa is required for particulate matter-induced cell death and lung inflammation. Faseb. J. 23, 2055–2064. [PubMed: 19237507]

Vaughan DE, Rai R, Khan SS, Eren M, Ghosh AK, 2017. Plasminogen activator inhibitor-1 is a marker and a mediator of senescence. Arterioscler. Thromb. Vasc. Biol. 37, 1446–1452. [PubMed: 28572158]

Vomund S, Schäfer A, Parnham MJ, Brüne B, von Knethen A, 2017. Nrf2, the master regulator of anti-oxidative responses. Int. J. Mol. Sci. 18, 2772.

Westrick RJ, Eitzman DT, 2007. Plasminogen activator inhibitor-1 in vascular thrombosis. Curr. Drug Targets8, 966–1002. [PubMed: 17896948]

Wu X, Pan B, Liu L, Zhao W, Zhu J, Huang X, Tian J, 2019. In utero exposure to PM2.5 during gestation caused adult cardiac hypertrophy through histone acetylation modification. J. Cell. Biochem. 120, 4375–4384. [PubMed: 30269375]

Xu Z, Li Z, Liao Z, Gao S, Hua L, Ye X, Wang Y, Jiang S, Wang N, Zhou D, Deng X, 2019. $PM_{2.5}$ induced pulmonary fibrosis in vivo and in vitro. Ecotoxicol. Environ. Saf. 171, 112–121. [PubMed: 30597315]

Yahata T, Ibrahim AA, Hirano KI, Muguruma Y, Naka K, Hozumi K, Vaughan DE, Miyata T, Ando K, 2021. Targeting of plasminogen activator inhibitor-1 activity promotes elimination of chronic myeloid leukemia stem cells. Haematologica106, 483–494. [PubMed: 32001531]

Yamaoka N, Murano K, Kodama H, Maeda A, Dan T, Nakabayashi T, Miyata T, Meguro K, 2018. Identification of novel plasminogen activator inhibitor-1 inhibitors with improved oral

bioavailability: structure optimization of N-acylanthranilic acid derivatives. Bioorg. Med. Chem. Lett28, 809–813. [PubMed: 29366646]

Yan R, Ku T, Yue H, Nan G, Sang N, 2020. PM2.5 exposure induces age-dependent hepatic lipid metabolism disorder in female mice. J. Environ. Sci. 89, 227–237.

Yang J, Chen Y, Yu Z, Ding H, Ma Z, 2019. The influence of $PM2_{.5}$ on lung injury and cytokines in mice. Exp. Ther. Med. 18, 2503–2511. [PubMed: 31572502]

Yue W, Tong L, Liu X, Weng X, Chen X, Wang D, Dudley SC, Weir EK, Ding W, Lu Z, Xu Y, Chen Y, 2019. Short term PM2.5 exposure caused a robust lung inflammation, vascular remodeling, and exacerbated transition from left ventricular failure to right ventricular hypertrophy. Redox Biol22, 101161. [PubMed: 30861460]

Zhu J, Zhu LWS, Yang JH, Xu YL, Wang C, Li ZY, Mao W, Lu DZ, 2018.Proteomic analysis of human umbilical vein endothelial cells exposed to PM2.5. J. Zhejiang Univ. - Sci. B19, 458–470.

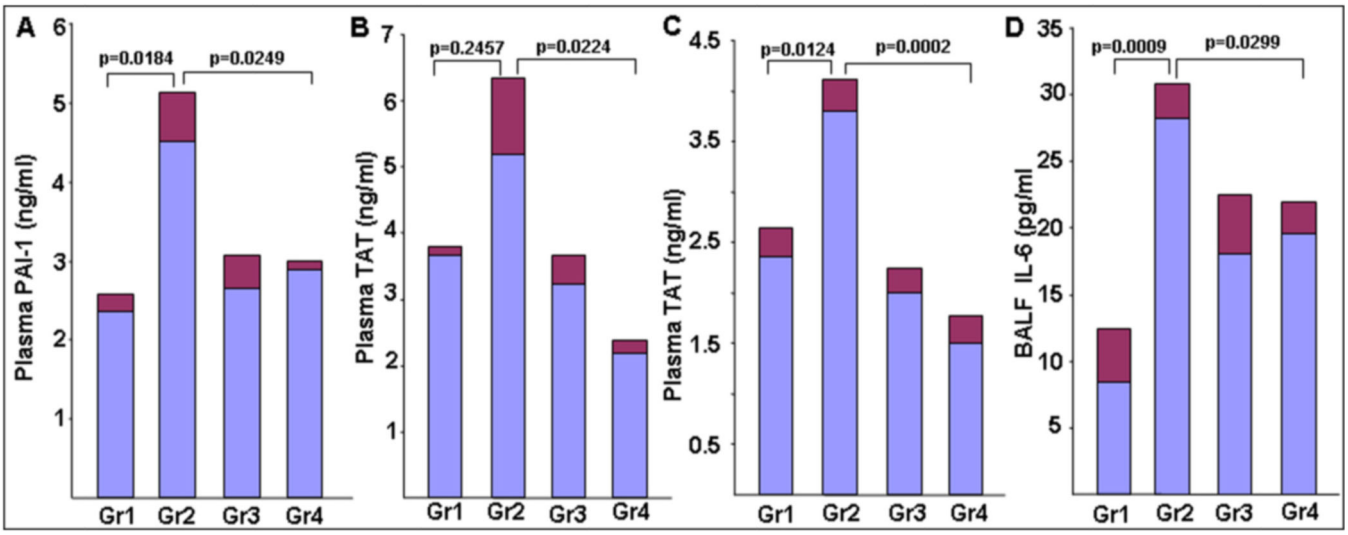

Fig. 1. PAI-1 inhibitor TM5614 inhibits the levels of $PM_{2.5}$-induced PAI-1 and TAT in plasma and IL-6 in BALF.

Plasma collected from 4 groups of mice (n = 4–8) was used in duplicate for PAI-1 and TAT assays. Day 1–6: TM5614 (10 mg/kg/day); Day 7: $PM_{2.5}$ (50 μg/mouse) or PBS intratracheal instillation; Day 8: Plasma collected and processed for PAI-1 (**A**) or TAT (**B**) assay using an ELISA kit. (**C**) TAT levels in plasma from mice after 72 h treatment with $PM_{2.5}$ (200 μg/mouse) and TM5614 (10 mg/kg/day) (n = 4–7). (**D**) IL-6 levels in BALF from mice after 24 h treatment with $PM_{2.5}$ (50 μg/mouse) and TM5614 (10 mg/kg/day) were determined in duplicate using an ELISA kit (n = 7–8). Data presented as Mean (blue bar) ± SEM (red bar). Gr1: PBS; Gr2: $PM_{2.5}$; Gr3: TM5614; Gr4: TM5614 + $PM_{2.5}$.

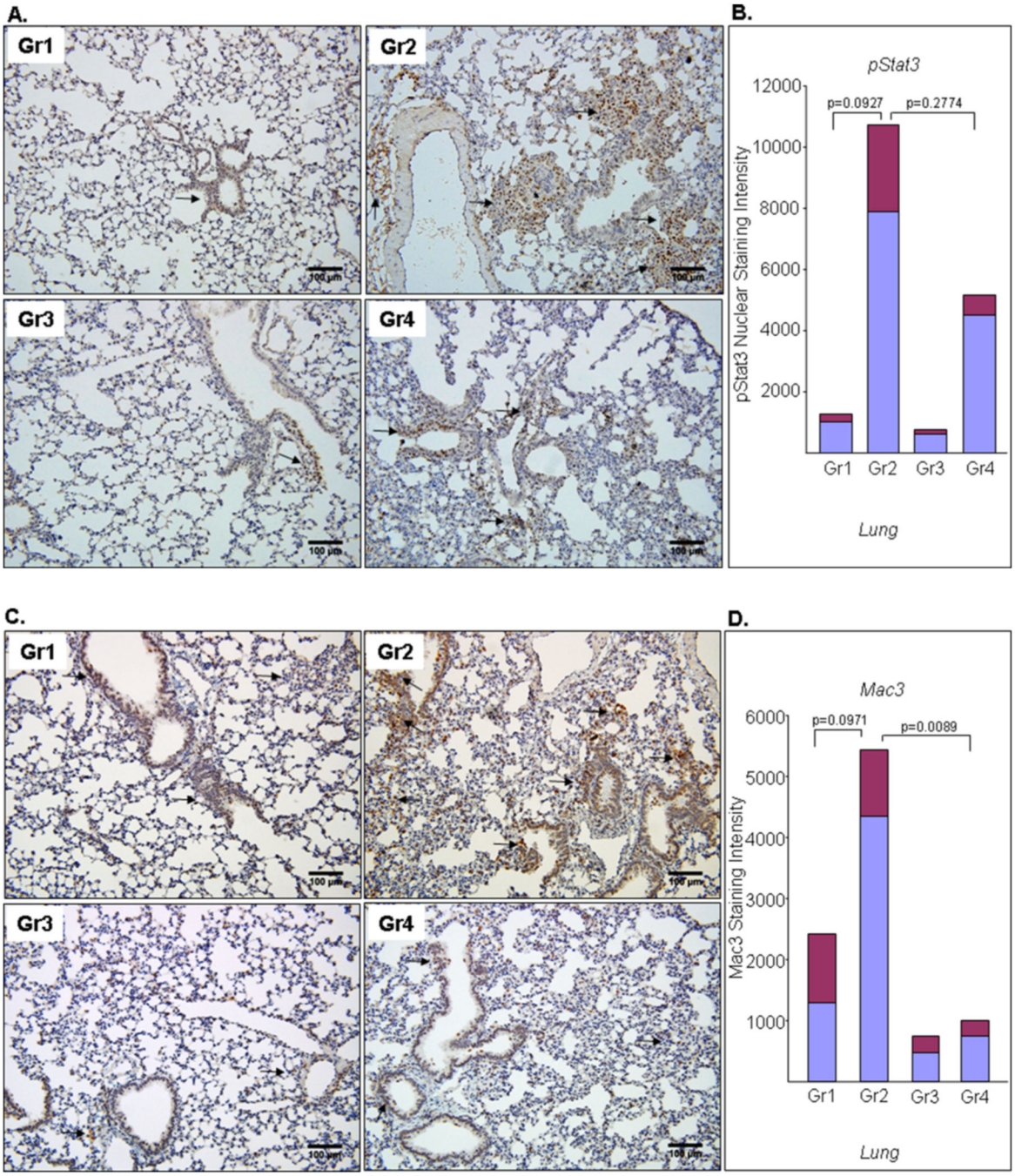

Fig. 2. Effect of PAI-1 inhibitor TM5614 on $PM_{2.5}$-induced inflammation in lungs.

Lungs collected from 4 groups of mice (n = 4–6) were processed for immunohistochemistry using anti-pSTAT3 antibody (A,B) and antiMac3 antibody (C,D). Day 1–6: TM5614 (10 mg/kg/day); Day 7: $PM_{2.5}$ (200 μg/mouse) or PBS instillation; Day 10: Lungs were collected and processed for immunohistochemistry. Representative images of pSTAT3 stained lung sections (**A**) and Mac3 stained lung sections (**C**) are shown. Images are reduced form of original 20X images. The levels of nuclear pSTAT3 in several fields of each lung section were determined by ImageJ software followed by statistical analysis. Quantitative

data are shown in (**B**) for pSTAT3 and (**D**) for Mac3. Data presented as Mean (blue bar) ± SEM (red bar). Gr1: PBS; Gr2: $PM_{2.5}$; Gr3: TM5614; Gr4: TM5614 + $PM_{2.5}$. Arrows indicate the presence of pSTAT3 (A) and Mac3 (B) positive cells.

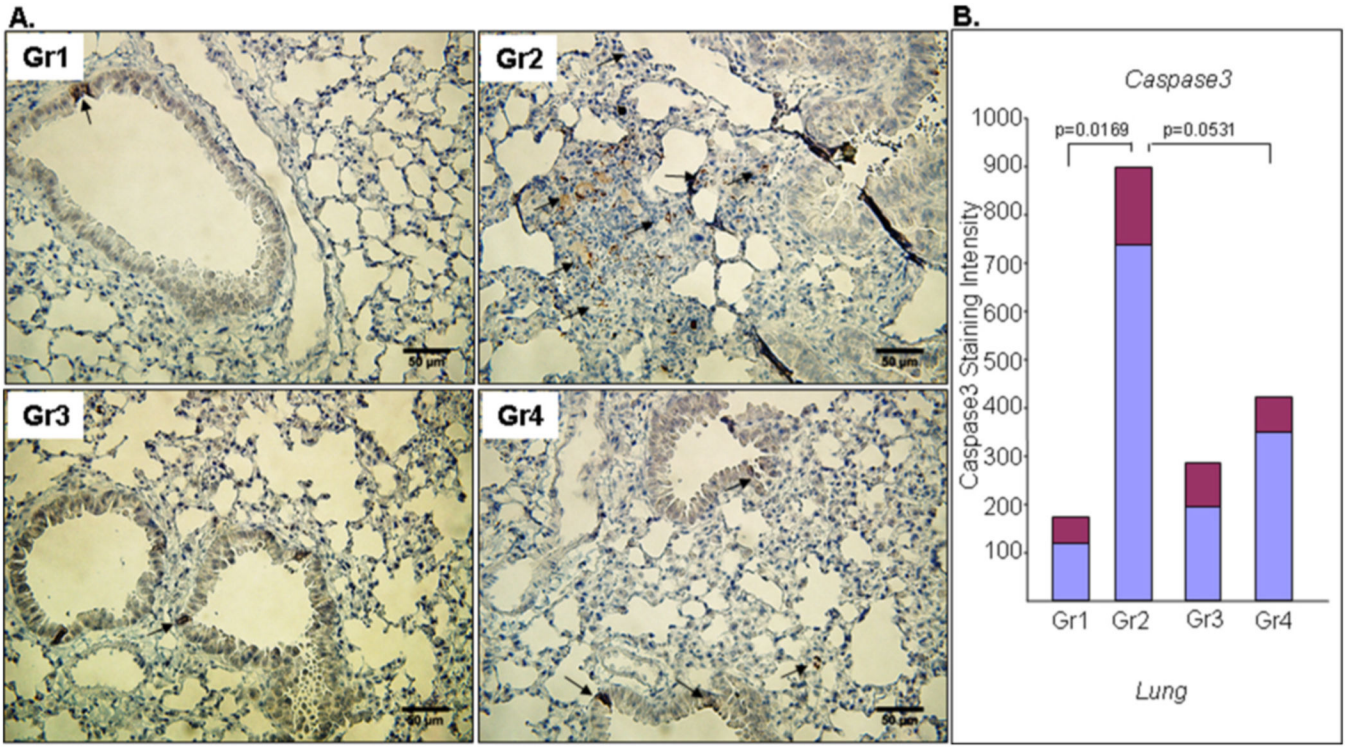

Fig. 3. Effect of TM5614 on $PM_{2.5}$-induced cellular apoptosis in lungs.

Lungs collected from 4 groups of mice (n = 4–6) were processed for immunohistochemistry using an anti-cleaved caspase 3 antibody. Mice were fed with TM5614 (10 mg/kg/day) for 6 days and on day 7, $PM_{2.5}$ (200 µg/mouse) instillation or PBS was used as control. After 72 h, lungs were processed for immunohistochemistry. Representative images are reduced form of original 40X images (**A**). The levels of cleaved caspase 3 in several fields of each lung were determined by ImageJ software. Quantitative data are shown in (**B**). Data are presented as Mean (blue bar) ± SEM (red bar). Gr1: PBS; Gr2: $PM_{2.5}$; Gr3: TM5614; Gr4: TM5614 + $PM_{2.5}$. Arrows indicate the presence of cleaved caspase 3 positive cells.

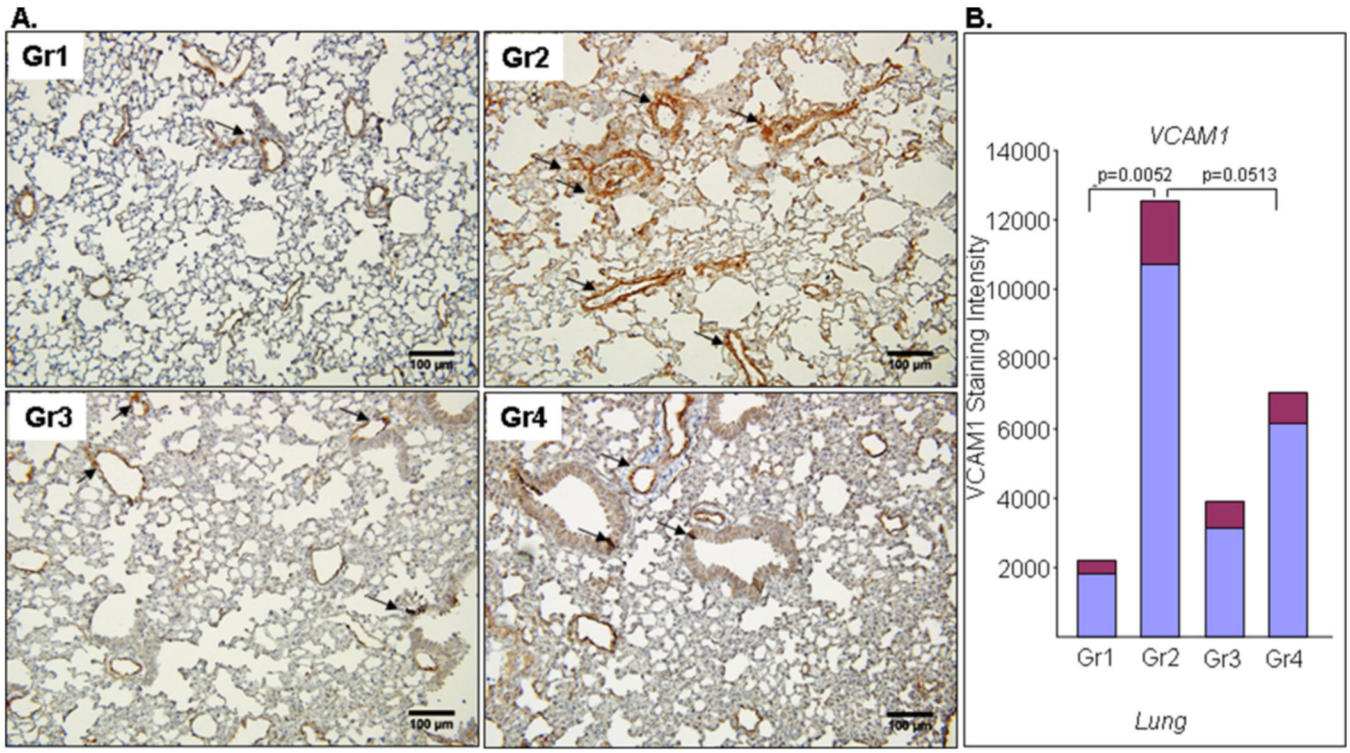

Fig. 4. TM5614 reduces $PM_{2.5}$-induced adhesion molecule VCAM1 in lungs.

Lungs collected from 4 groups of mice (n = 4–6) were processed for immunohistochemistry using an anti-VCAM1 antibody. Day 1–6: TM5614 (10 mg/kg/day); Day 7: $PM_{2.5}$ (200 µg/mouse) or PBS instillation; Day 10: Lungs were processed for immunohistochemistry. Representative images are reduced form of original 20X images (**A**). The levels of VCAM1 in several fields of each lung were determined by ImageJ. Quantitative data are shown (**B**). Data are presented as Mean (blue bar) ± SEM (red bar). Gr1: PBS; Gr2: $PM_{2.5}$; Gr3: TM5614; Gr4: TM5614 + $PM_{2.5}$. Arrows indicate the presence of VCAM1 positive sites.

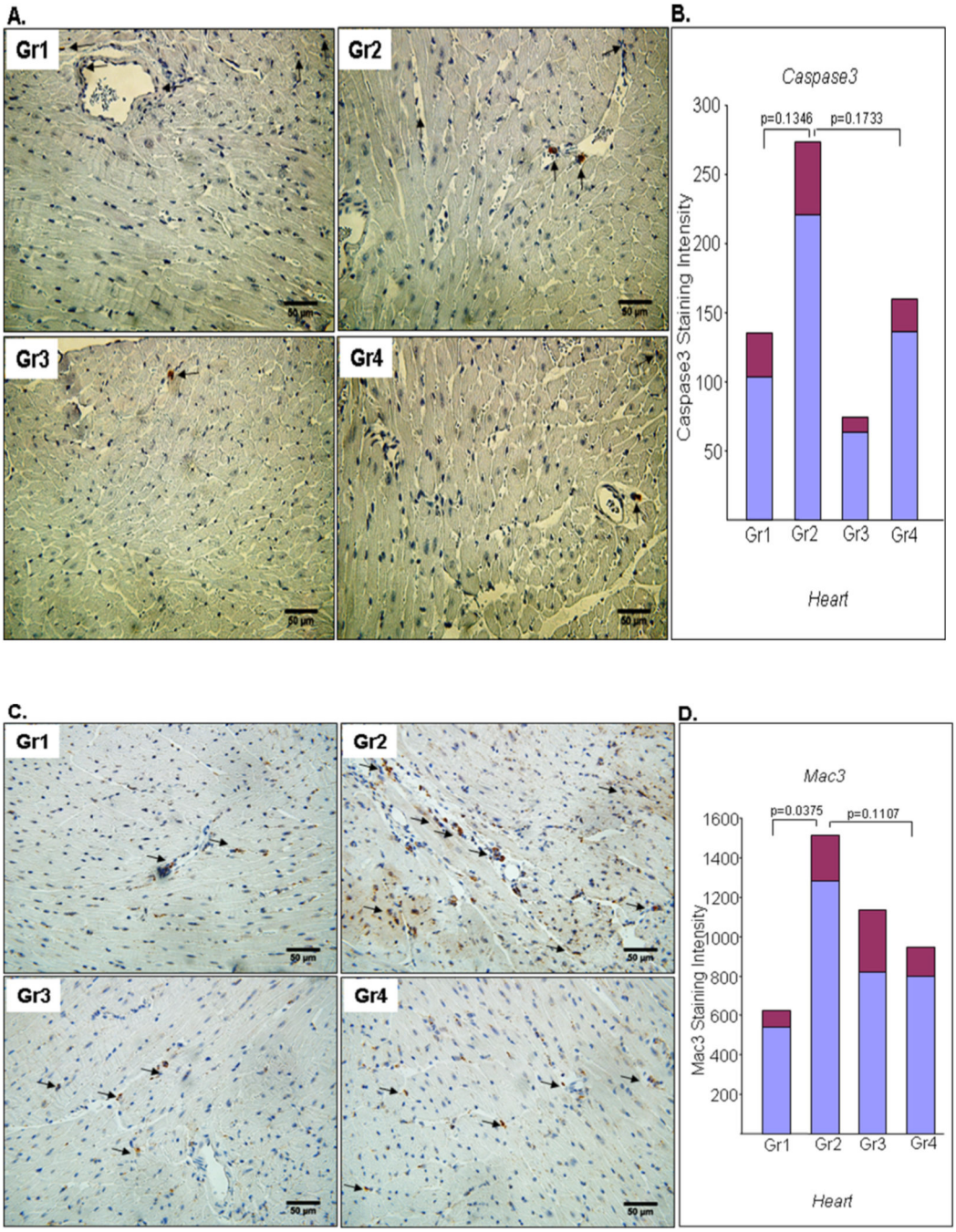

Fig. 5. Effect of PAI-1 inhibitor TM5614 on $PM_{2.5}$-induced cellular apoptosis and inflammation in hearts.

Hearts collected from 4 groups of mice (n = 4–6) were processed for immunohistochemistry using an anti-cleaved caspase 3 antibody (**A**) and anti-Mac3 antibody (**C**). Day 1–6: TM5614 (10 mg/kg/day); Day 7: $PM_{2.5}$ (200 μg/mouse) or PBS instillation. After 72 h, hearts were collected and processed for immunohistochemistry. Representative images are reduced form of original 40X images. The levels of cleaved caspase 3 and Mac3 in several fields of each heart section were determined by ImageJ. Quantitative data are shown in (**B**)

for cleaved caspase 3 and (**D**) for Mac3. Data are presented as Mean (blue bar) ± SEM (red bar). Gr1: PBS; Gr2: $PM_{2.5}$; Gr3: TM5614; Gr4: TM5614 + $PM_{2.5}$. Arrows indicate the presence of cleaved caspase 3 (**A**) and Mac3 (**C**) positive cells.

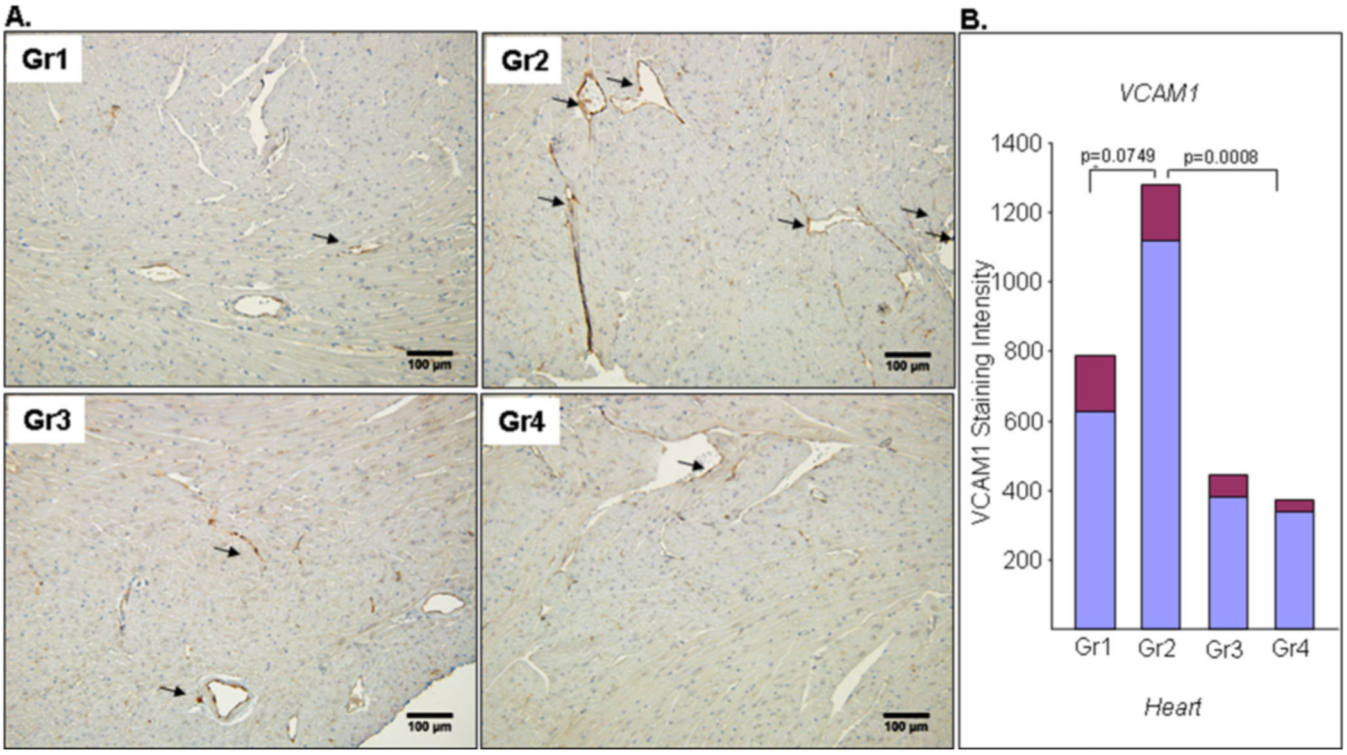

Fig. 6. TM5614 reduces $PM_{2.5}$-induced adhesion molecule VCAM1 in hearts.

Hearts collected from 4 groups of mice (n = 4–6) as indicated were processed for immunohistochemistry using an anti-VCAM1 antibody. Day 1–6: TM5614 (10 mg/kg/day); Day 7: $PM_{2.5}$ (200 µg/mouse) or PBS instillation; Day 10: Heart sections were processed for immunohistochemistry. Representative images are shown in (**A**). Images are reduced form of original 20X images. The levels of VCAM1 in several fields of each heart were determined by ImageJ software. Quantitative data are shown in (**B**). Data are presented as Mean (blue bar) ± SEM (red bar). Gr1: PBS; Gr2: $PM_{2.5}$; Gr3: TM5614; Gr4: TM5614 + $PM_{2.5}$. Arrows indicate the presence of VCAM1 positivity.

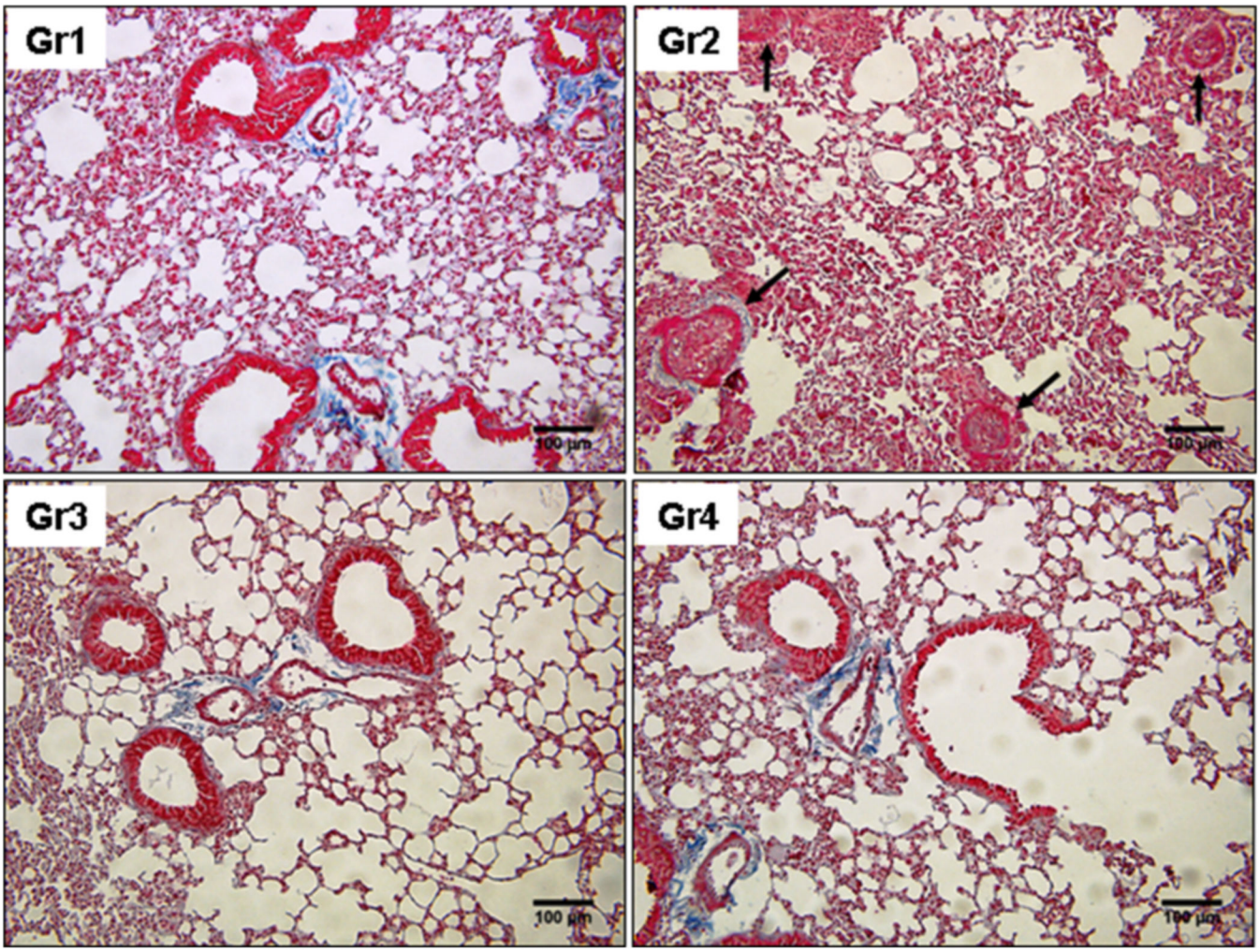

Fig. 7. $PM_{2.5}$ induces pulmonary thrombosis and PAI-1 inhibitor TM5614 prevents lung thrombogenesis.

Mice were divided into 4 groups (n = 4–7). In Group1, mice were fed with regular chow and received PBS. In Group 2, mice were fed with regular chow and received $PM_{2.5}$ (100 μg/mouse/once per week for 4 weeks). In Group 3, mice were fed with chow containing TM5614 (10 mg/kg/day) for 6 days and then received PBS. In Group 4, mice were fed with chow containing TM5614 (10 mg/kg/day) for 6 days and then received $PM_{2.5}$ (100 μg/mouse/once per week for 4 weeks). Representative image from each group are shown. Images are reduced form of original 20X images. An arrow indicates the presence of a thrombus.

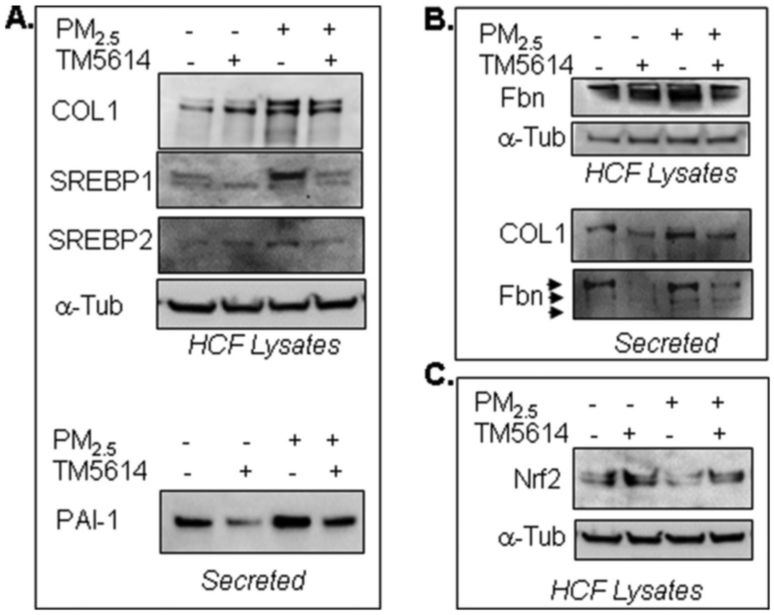

Fig. 8. TM5614 blocks $PM_{2.5}$-induced cellular stress and profibrogenic responses.

Human cardiac fibroblasts (HCF) were cultured in 12-well clusters. After 24 h, media were replaced with 0.1% FBS containing DMEM for 3 h. Cells were pretreated with TM5614 (10 μM) or DMSO (vehicle control) for 2 h followed by treatment with $PM_{2.5}$ (50 μg/ml) in triplicate for another 2 h. Supernatants and cell lysates were used for western blotting using antibodies as indicated (**A**). In (**B**) and (**C**), cells were pretreated with TM5614 (10 μM) or DMSO in triplicate. After 24 h, media were replaced with 0.1% FBS containing DMEM and treated with TM5614 (10 μM) or DMSO and $PM_{2.5}$ (50 μg/ml) in triplicate for another 24 h. Supernatants and cell lysates were processed for western blotting using antibodies as indicated (**B, C**). Fbn: fibronectin; COL1: Type 1 collagen; α-Tub: α-Tubulin.

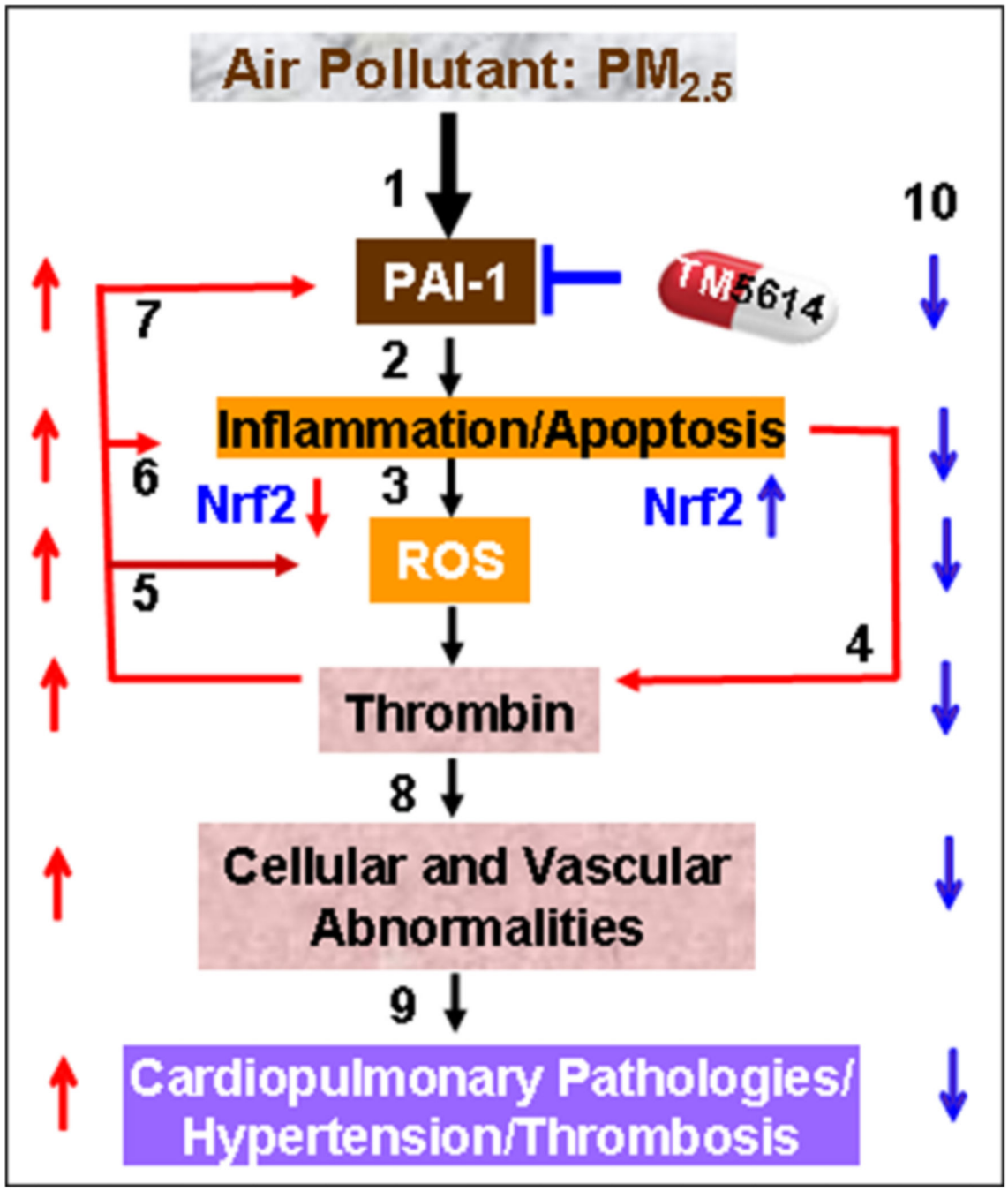

Fig. 9. Possible pathological pathways driven by $PM_{2.5}$-induced PAI-1 and the beneficial effect of PAI-1 inhibitor TM5614.

Air pollution stressors increase the levels of proinflammatory and prothrombotic mediators/regulators that cause cellular and vascular dysfunction and contribute to cardiopulmonary vascular pathologies. Neutralization of $PM_{2.5}$-induced PAI-1 with TM5614 reduces $PM_{2.5}$-induced cardiopulmonary vascular pathologies. In the depicted model, the individual step and feed-back loop are supported by the present study and or previous published works by other investigators. **1.** Air-pollutant: $PM_{2.5}$ increases the level of PAI-1 (present study

and Upadhyay et al., 2010; Budinger et al., 2011); **2**. PAI-1 increases inflammation and apoptosis (This study and Kubala et al., 2018); **3**. Inflammation increases ROS (Mittal et al., 2014); **4**. Inflammation induces thrombin (Margetic S. 2012, Foley and Conway, 2016); **5**. Thombin induces the levels of ROS (Carrim et al., 2015); **6**. Thrombin increases inflammation/apoptosis (Lopez et al., 2007; Chen and Dorling, 2009; Danckwardt et al., 2013; Foley and Conway, 2016); **7**. Thrombin increases PAI-1 level (Hsieh et al., 2019); **8**. Thrombin induces cellular and vascular abnormalities (present study and Rabiet et al., 1994); **9**. Increased cellular dysfunction, elevation of thrombin-induced fibrinogen to fibrin deposition leads to cardiopulmonary pathologies, hypertension, thrombosis (present study and Savoia et al., 2011), **10**. The results of the present biochemical, histological, immunohistological and cellular studies provide evidence on the pivotal role of air-pollutant $PM_{2.5}$-induced PAI-1 in cardiopulmonary vascular pathologies, and the efficacy of a novel PAI-1 inhibitor TM5614 in improving air pollutant-induced cardiopulmonary vascular pathologies. Red upward arrow indicates induction of pathological factors by air-pollutants. Red downward arrow indicate downregulation of anti-pathological factor. Blue downward arrow indicates amelioration of pathological events by PAI-1 inhibitor TM5614. Blue upward arrow indicates upregulation of anti-pathological factor.

Table 1

Experimental design, endpoint measurements and results of each experimental condition.

Mice were fed with TM5614 chow or normal chow for 6 days followed by treatment with PBS or $PM_{2.5}$ for 24 h (A) or 72 h (B) or 4 weeks (C) in the presence and absence of TM5614. Wildtype (PAI-$1^{+/+}$), heterozygous (PAI-$1^{+/-}$) and knockout (PAI-$1^{-/-}$) mice were treated with PBS or $PM_{2.5}$

for 4 weeks (D). Effect of TM5614 on $PM_{2.5}$-induced cellular stress and abnormalities (E). Gr1:Group1; Gr2: Group 2; Gr3: Group 3; Gr4: Group 4. Expression levels: +/+ > + > +/− > −.

Pharmacologic Inhibition of PAI-1	Endpoint Measurements	Results				Sections
		Gr1 PBS	Gr2 $PM_{2.5}$	Gr3 TM5614	Gr4 $PM_{2.5}$+ TM5614	
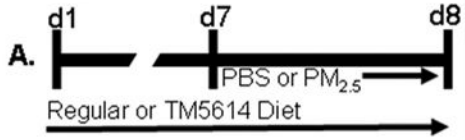	Plasma: PAI-1, Thrombin BAL Fluid: IL-6	+/-	++	+/-	+	3.1 & 3.2
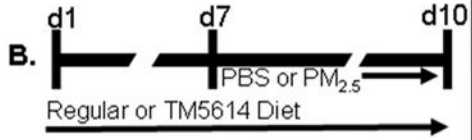	Thrombin, Heart and Lung tissues: Mac3, pSTAT3, Caspase3, VCAM-1	+/-	++	+/-	+	3.1,3.3 & 3.4
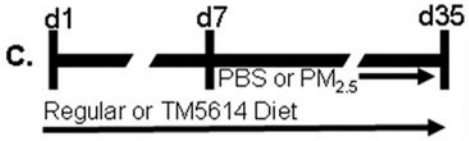	Systolic and Diastolic Blood pressure, Cardiac Hypertrophy, Vascular Thrombosis	+/-	++	+/-	+	3.5 & 3.6
Genetic deficiency of PAI-1	**Endpoint Measurements**	**Results**				**Sections**
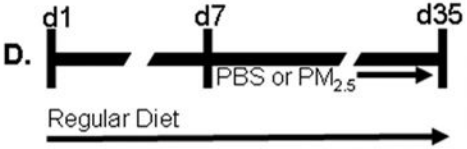	Lung tissue: Thrombosis	PAI-1+/+ PBS	PAI-1+/+ $PM_{2.5}$	PAI-1+/- PBS	PAI-1+/- $PM_{2.5}$	PAI-1-/- PBS	PAI-1-/- $PM_{2.5}$	3.7
		-	++	-	+/-	-	++	
PAI-1 Inhibition in Cellular Model	**Endpoint Measurements**	**Results**				**Sections**
		DMSO	TM5614	$PM_{2.5}$	$PM_{2.5}$+TM5614	
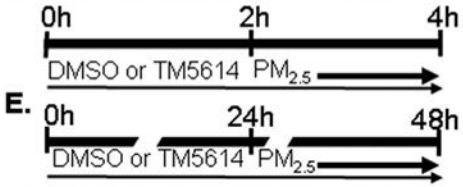	Collagen, PAI-1, SREBP1, SREBP2,	+/-	+/-	++	+/-	3.8
	Collagen, Fibronectin	+/-	+/-	++	+/-	
	Nrf2	+	+	-	+	